Technical Note

Dynamic Observation of Hydrogen-Induced Cracking in Medium Carbon Martensitic Steel†

Yan TIAN*, Hiroji NAKAGAWA** and Fukuhisa MATSUDA***

KEY WORDS: (Cold Cracking) (Hydrogen Embrittlement) (High Strength) (Electron Microscope)

Welding of medium carbon low alloy steel is generally very difficult, because it has very high susceptibility to hydrogen-induced cold cracking in welding due to high hardenability. Thus, direct dynamic observation of the hydrogen-cold cracking with scanning electron microscope (SEM) and Nomarski differential interference microscope[1] has been tried in order to reveal the behavior of the cold cracking in this type of steel.

Material used is Ni-Cr steel JIS SNC631 whose chemical composition is shown in **Table 1**. Two types of specimens were cut from the material of original 150mm diameter rod and prepared for dynamic observation. The first type is shown in **Fig. 1(a)**, to which hydrogen was charged at 950°C in Ar + 10%H_2 atmosphere for 1 hr, and then was quenched in iced water. The diffusible hydrogen content measured with gas chromatographic method was 1.6ml/100g. The second type is welded one shown in **Fig. 1(b)**, which was prepared by the following procedure: At first a block was cut from the material, which had 60mm in length, 28mm in width and 15mm in thickness, and TIG-arc bead-on-plate welding with Ar + 0.5%H_2 shielding gas was done on the block without filler wire. Welding conditions were; welding current of 150A, arc voltage of 20V and welding speed of 150mm/min. In this condition the cooling time from 800 to 500°C was about 9sec. When the temperature of weld zone was cooled to 100°C, the block was quenched in iced water and then preserved in liquid nitrogen. The diffusible hydrogen content was 0.9 ml/100g. After that, several pieces shown in Fig. 1(b) were mechanically cut from the block.

Both types of specimens were metallographically polished as soon as possible and set to a testing device utilizing bending method which is described elsewhere[1-3]. The direction of bending stress is shown in Fig. 1. The specimen set to the testing device was put on the stage of Nomarski microscope or in the vacuum chamber of SEM, and dynamic observation was soon started. SEM image was recorded with VTR.

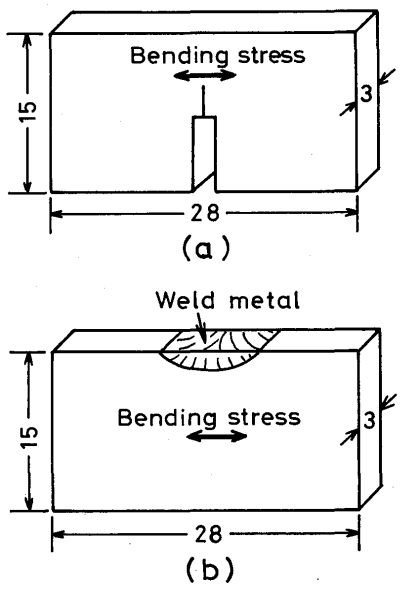

Fig. 1 Specimen configuration for dynamic observation

Table 1 Chemical composition and mechanical properties after annealing at 600°C of SNC 631

Composition (wt.%)							σ_Y	σ_T
C	Si	Mn	P	S	Ni	Cr	(kgf/mm^2)	(kgf/mm^2)
0.30	0.27	0.47	0.010	0.020	2.64	0.83	78	90

† Received on September 30, 1982

* Visiting Research Scholar (Lecturer, Mechanical Engineering Department, Tsing Hua University, Peking, China)
** Research Instructor
*** Professor

Transactions of JWRI is published by Welding Research Institute of Osaka University, Ibaraki, Osaka, Japan

By the way, the Vickers hardness of the specimen shown in Fig. 1(a) was about 400, and the maximum hardness of coarse-grained region in HAZ in Fig. 1(b) was about 430.

An example of SEM observation of the specimen in Fig. 1(a) is shown in **Fig. 2.** In Fig. 2(a) large plastic deformation (white lines in Photo) and cracks (dark lines) develop discontinuously from the tip of the notch. There are two growing crack tips in parts A and B. The part A is magnified in Fig. 2(b), which shows some straight plastic deformation lines and a straight microcrack paralleling them. Microetching after the observation revealed that both of them occurred along martensite laths.

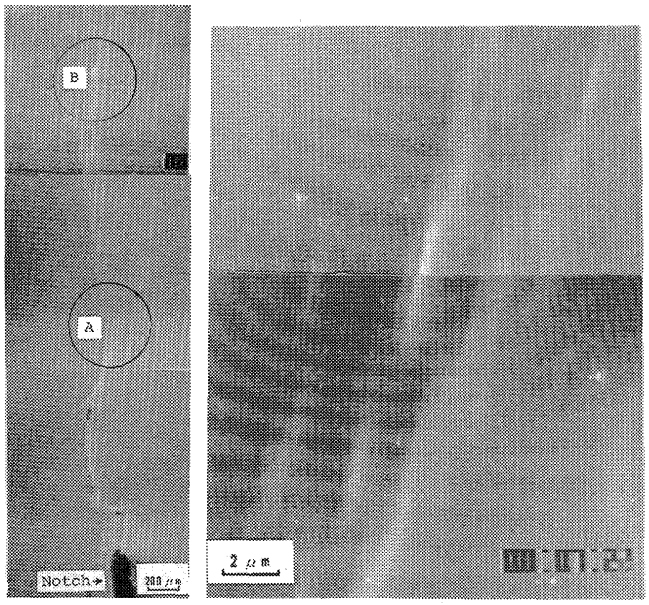

(a) low magnification (b) high magnification of part A

Fig. 2 Plastic deformation and transgranular microcrack in the specimen in Fig. 1(a) (SEM observation)

Another interesting example is shown in **Fig. 3,** where the line outside the figure give the position of a prior austenite grain boundary, and arrows give the direction of bending stress. Thus it can be understood that plastic deformation occurs along grain boundary and intergranular microcracks discontinuously occur nearly perpendicular to the bending stress. The same characteristics are well observed in **Fig. 4** in a low magnification. These behaviors are very interesting, because they show the necessity of both plastic deformation which has been often mentioned in many reports[4] and normal stress for initiation of hydrogen-induced crack.

Then, the microcrack in HAZ in Fig. 1(b) was connected with sulphide as described in the following.

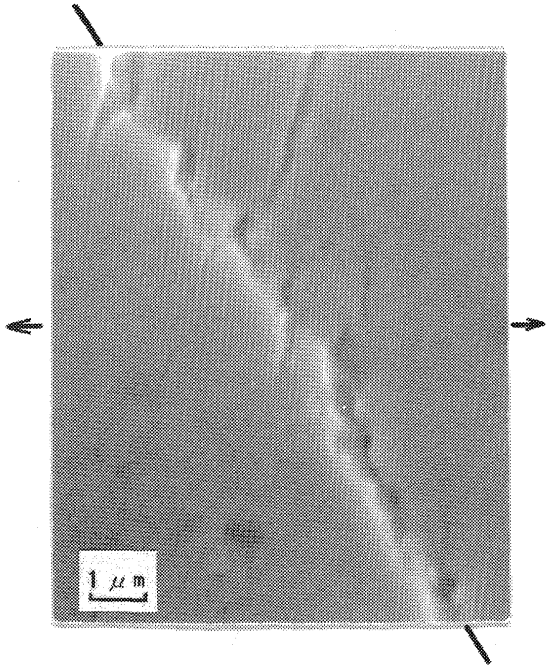

Fig. 3 Intergranular plastic deformation and microcrack in the specimen in Fig. 1(a) (SEM observation)

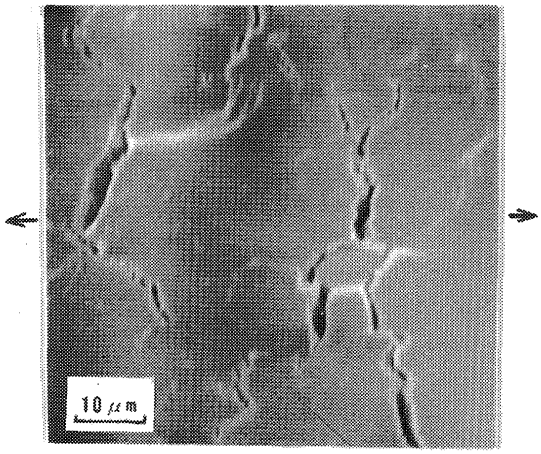

Fig. 4 The same phenomena in a low magnification as in Fig. 3 (SEM observation)

For example, **Fig. 5(a)** shows several microcracks along grain boundaries in coarse-grained region near the fusion boundary, and observation in a higher magnification, **Fig. 5(b)** , reveals the existence of sulphides A, B and C at the grain boundary. These sulphides penetrated into grain boundary due to liquation in partially melted region. Also it was noticed that plastic deformation prior to cracking was comparatively less than in Fig. 3. It is considered to be the reason that the interface between penetrated sulphide and matrix is active hydrogen-trapping site.

In spherodized region in HAZ, there was a nonuniform distribution in hardness because of nonuniform distribution of carbon content due to relatively short thermal cycle in low peak temperature. Namely,

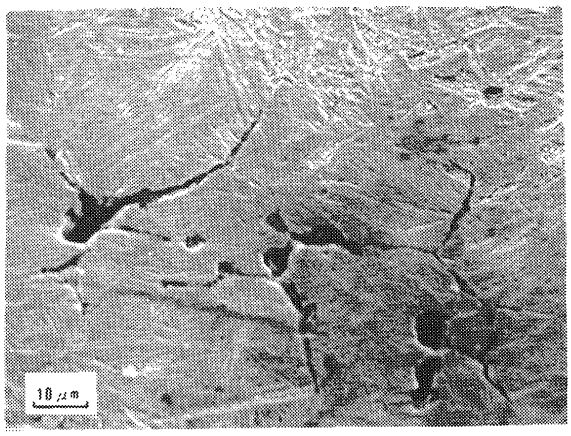

(a) low magnification

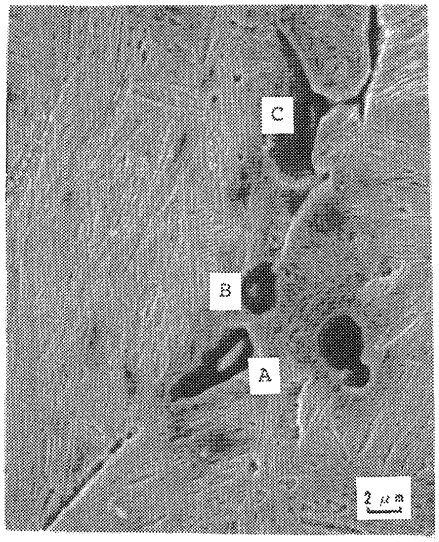

(b) high magnification

Fig. 5 Microcrack at grain boundary to which sulphide penetrated in partially melted region in the specimen in Fig. 1(b)

although the mean hardness was Hv 410, the peak hardness reached about 600. This part was susceptible to intergranular microcrack, and the microcrack was frequently conneted with sulphide as seen in **Fig. 6.**

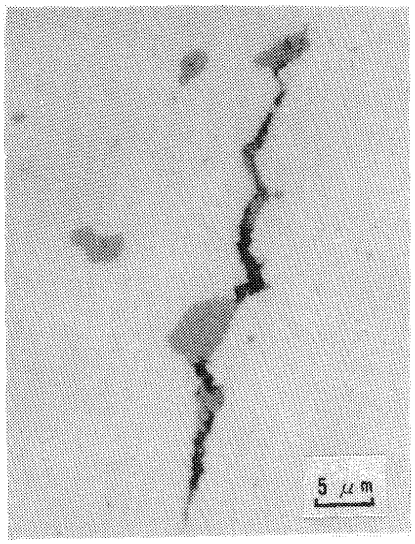

Fig. 6 Microcrack and sulphide in spherodized region in the specimen in Fig. 1(b)

The direct observation technique has conduced to interesting appreciation of hydrogen-induced cracking. Namely, the necessity of plastic deformation and normal stress for crack initiation, and noticeable effect of sulphide on crack initiation have been well understood. At present, however, it is difficult to interpret the behaviors of both specimens systematically. Further study in due consideration of the effect of themal cycle on sulphide and microstructure is a future subject.

References

1) F. Matsuda, etal: Trans. JWRI, Vol. 8 (1979), No. 2, p. 289.
2) F. Matsuda, etal: Trans. JWRI, Vol. 8 (1979), No. 2, p. 293.
3) F. Matsuda, etal: Trans. JWRI, Vol. 10 (1981), No. 1, p. 81.
4) For, example, M. Nagumo, etal: J. Japan Inst. Met., Vol. 45 (1981), No. 12, p. 1309.